Risk Analysis of an Autonomous Surface Craft for Operation in Harsh Ocean Environments

Zhi Li, Ralf Bachmayer
Department of Ocean and Naval Architectural Engineering
Memorial University of Newfoundland
St. John's, Canada
zhi.limun@gmail.com
bachmayer@mun.ca

Andrew Vardy
Department of Computer Science and
Department of Electrical and Computer Engineering
Memorial University of Newfoundland
St. John's, Canada
av@mun.ca

***Abstract*—Risk analysis of an Autonomous Surface Craft (ASC) is a very important subject since it is closely related to the safety of an ASC operating in harsh ocean environments. In this study, we provide a detailed analysis of the primary disturbance of ocean waves and its influence on an ASC's roll motion. A conventional decoupled nonlinear roll motion model has been chosen and through experiments the roll motion model parameters are successfully identified. Using this model, we perform extensive simulations under different assumed wave conditions. Our analysis is based on the well-known erosion basin technique in phase plane. The safe region proportion has been defined to serve as a safety criterion. Through analysis, we find out that the safety of an ASC operating in the ocean is related to the wave amplitude and wave encounter frequency. This relationship provides a useful reference for risk analysis of an ASC. The results provided can be regarded as guidelines for an ASC's safety determination, and thus they are planned to be integrated into an ASC for its self safety awareness. The presented method can also be extended to other medium-size or large marine vessels for their operational safety analysis.**

Keywords*—Autonomous Surface Craft; risk analysis; erosion basin

I. INTRODUCTION

There is an increasing interest for deployment of Autonomous Surface Craft (ASC) in different ocean exploration missions [1]–[5]. However, an ASC operating on the ocean surface has to be able to survive fast-changing ocean environments, i.e. strong winds and waves. A fundamental question is how we can assess in real-time the vehicle's safety with respect to different adverse ocean influences. This is a prerequisite for a successful ASC mission. An ASC operating in the seaway normally has 6 DOF motion, and the oscillatory motions in roll, pitch and heave may lead to the vehicle capsizing. In this study, the risk analysis of an ASC has been discussed. We concentrate our analysis on the nonlinear rolling motion, but the proposed method can also be extended for an ASC's pitching or heaving safety analysis. An ASC's horizontal motion modeling and analysis for controlling purposes has been extensively addressed [3], [6], [7], but it is the mostly uncontrolled motions, roll, pitch and heave, that are the most critical for vehicle safety. Therefore, this study provides a unique supplement for the ASC research community.

Nonlinear ship rolling motion analysis traces back to 1970s [8], and it has been a research topic since then because it is closely related to the vessel stability against capsizing in the seaway. The rolling motion is conventionally decoupled from the other degrees of freedom, and the roll exciting moments are normally assumed to be from the harmonic waves. The nonlinearity in the roll motion leads to some well-known complicated phenomena, such as jumping and system chaos. For instance, due to the nonlinearity of the roll restoring moments, the region around the roll resonant frequency may have multiple steady-state roll response solutions [9]. To investigate the nonlinear roll dynamics and perform the risk analysis, many approaches have been developed. In the early days, due to the limitation of computational power, the analytical approximations of the steady-state rolling response solutions were formulated. Some typical analytical methods include Perturbation Method and Harmonic Balance Method [10], and they have demonstrated their effectiveness in the main rolling resonance region. The Melnikov method [11], [12] has been widely accepted and employed for analysing the ship rolling dynamics analysis. As a global analysis technique, it assumes that the ship roll motion is subjected to a harmonic excitation. Through calculating the value of the Melnikov function, the distance between the stable and unstable manifolds can be determined as a criteria for prediction of the system chaotic behaviour. In [13], the Melnikov method has also been extended for taking into account strong damping effects.

Taking advantage of the recent advances in computing power, numerical methods have been extensively employed for analysing the ship nonlinear roll motion and even the complex coupled motions in the seaway. In this study, we will implement the erosion basin technique [14], [15] to investigate the nonlinear roll dynamics of an ASC in regular seas. The concept of the safe basin was firstly introduced in [16], and it was based on the phase plane analysis [17] where the evolution of the roll motion, i.e. roll angle and roll rate, are plotted on a 2D plane. It has been demonstrated by several researchers [8] that with the increment of the wave exciting amplitude, the area of the safe basin will reduce or erode. When this happens, the probability of a ship capsizing through rolling increases. The erosion basin method is advantageous because it does not need to assume the low wave excitation and small damping effects as is required by the Melnikov method. Moreover, due to the roll nonlinearity, the dynamic behaviour of the roll motion is sensitive to initial conditions. The erosion basin method examines all possible initial conditions, and thus can provide

an accurate estimation of the roll motion stability. There are also some other methods including Lyapunov and bifurcation analysis that have been researched, and interested readers can refer to [8].

In this paper, we investigate an ASC's nonlinear roll motion risk analysis based on different wave conditions. An accurate roll motion model is experimentally identified, based on which extensive simulations are carried out. As far as the authors are concerned, the risk analysis for an ASC has not been investigated yet, and thus we employ the well-accepted erosion basin technique for the nonlinear dynamics analysis. The outcome of the research can assist us in determination of an ASC's risk/safety for a specific mission, and it is planned that the corresponding results will be integrated into an ASC's autonomous guidance system to improve its self safety awareness. The paper is organized as follows. Section II describes roll motion modeling for the studied ASC, and the nonlinear motion model parameters are identified through tank tests. In Section III, the risk analysis of the ASC's roll motion is provided. Extensive simulations based on the erosion basin technique has been implemented and the results are summarized for rolling motion safety determination. Section IV presents our conclusion and future work.

II. ROLL MOTION MODELING AND PARAMETER IDENTIFICATION

A. Roll Motion Model

Although in reality an Autonomous Surface Craft (ASC) operating in the seaway moves in all six degrees of freedom simultaneously, for the sake of simplicity, we follow the convention to decouple the roll motion from the other degrees of freedom. The nonlinear roll motion model is formulated as

$$I_r\ddot{\phi} + D(\dot{\phi}) + R(\phi) = K \tag{1}$$

where ϕ denotes the roll angle, I_r is the virtual roll moment of inertia that includes the added mass effect, $D(\dot{\phi})$ includes the nonlinear damping terms that is nonlinear and $R(\phi)$ represents the roll restoring moments. Eq. 1 has been widely employed for ship rolling motion and capsizing study in the naval architectural community [8], [10], [12], [14], [15]. However, it is worth noting that the hydrodynamic coefficients are generally wave frequency dependent. In the scope of this study, the condition of regular wave excitation and small-amplitude response is assumed. Hence, the hydrodynamic coefficients can be treated as constant. In Eq. 1, K is the external excitation moment and it may include the disturbances from the ocean environments such as wind, waves and ocean currents. The studied ASC only has a relatively small portion above the water, so the wind effect is negligible. The ocean current can be regarded as constant or slowly changing compared to the roll dynamics in the vehicle's translational motion, thus it can be neglected for the oscillatory motion. Therefore, we can assume the main contribution for the roll excitation moments is from the waves.

The damping moments are normally formulated as a linear, linear plus quadratic or linear plus cubic form polynomial [18]. In this study, we employ the form of linear plus quadratic term, which is given as

$$D(\dot{\phi}) = D_1\dot{\phi} + D_2\dot{\phi}|\dot{\phi}| \tag{2}$$

where D_1 and D_2 are linear and quadratic damping coefficients. The restoring moments can be regarded as a linear function of ϕ within the small range of the equilibrium position. However, when the displacement angle is large, the relationship is nonlinear and it is normally formulated as an odd polynomial as

$$R(\phi) = R_1\phi + R_3\phi^3 + R_5\phi^5... \tag{3}$$

A full derivation of the wave exciting moments for roll motion can be found in [19], and here we only provide a brief overview. The dimension of the studied ASC is Length×Width=1.5 m×1.0 m and we are considering the wind waves that have a wavelength of over 10 m. Since the size of the ASC is small compared to the wavelength, we can apply the Froude-Krylov hypothesis. Thus, the wave exciting moment is calculated by integration of the wave pressure p_w acting on the surface S_B of the ASC hull as

$$\overrightarrow{M}_w^{FK} = \iint_{S_B} p_w(\overrightarrow{r} \times \overrightarrow{n})dS \tag{4}$$

where $\overrightarrow{r}$ is the position vector of a unit area on the hull body with respect to the center of gravity, $\overrightarrow{n}$ is the unit normal vector on the body surface directed into the body and

$$p_w = \varphi_w\rho\zeta_A\omega_w\sin(\omega_w t). \tag{5}$$

Note that in Eq. 5, φ_w is the potential of fluid velocities contributed from the sinusoidal wave on an ASC's body, ρ is the fluid density, ω_w is the wave frequency, ζ_A is the wave amplitude and t denotes the time. Based on Eq. 4, the roll excitation moment about the center of gravity can be derived as [20]

$$K = \rho g V_0 k\zeta_A\overline{GM}\sin(\chi)\sin(\omega_w t) \tag{6}$$

where $\overline{GM}$ is the metacentric height and can be regarded as constant, g is the gravitational acceleration, V_0 is the ASC displacement volume, k is the wave number and χ is the direction of the waves with respect to the heading direction of the ASC. Based on Eq. 6, a compact form representation can be formulated as

$$\begin{aligned} K &= I_r\alpha_A\omega_n^2\sin(\chi)\sin(\omega_w t) \\ &= K_0\sin(\omega_w t) \end{aligned} \tag{7}$$

where ω_n is the roll natural frequency, α_A is the amplitude of wave slope

$$\alpha_A = k\zeta_A$$

and K_0 is the wave excitation amplitude that is given as

$$K_0 = I_r\alpha_A\omega_n^2\sin(\chi). \tag{8}$$

If an ASC operates with a total velocity of U with respect to the mean water current in the horizontal plane, ω_w in the oscillatory term $\sin(\omega_w t)$ of Eq. 7 needs to be substituted by the wave encounter frequency ω_e as

$$\omega_e = \omega_w - \frac{\omega_w^2 U}{g}\cos(\chi).$$

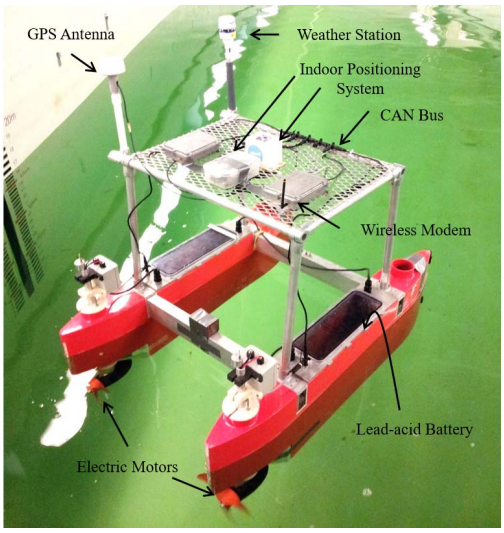

Fig. 1. Preliminary tests of the ASC SeaCat in the tow tank of Memorial University of Newfoundland.

B. Model Parameter Identification

The Autonomous Surface Craft (ASC) SeaCat shown in Fig. 1 is used in this study. SeaCat is a catamaran-type ASC that is developed for offshore scientific missions and a detailed description of the mechanical and electrical system design and payload sensors can be found in [21].

Free decay tests are carried out to collect the ASC motion data for the parameter identification in Eq. 1. The ASC SeaCat is put into the tank, and then external force is applied on the vehicle to introduce a static roll displacement. When the external force is removed, the vehicle roll oscillations will decay until the motion levels out around the equilibrium position. We employ the Attitude and Heading Reference System (AHRS) for measurement of the roll angle. The sampling rate of the sensor is 100 Hz. The AHRS is configured to output Euler angles with an angular measurement accuracy of $\pm 0.5^{\circ}$.

Some system properties have been summarized in Table I, where I_r is estimated based on the collected decay data and $\overline{GM}$ is experimentally determined through performing the ASC inclining tests and the value has also been validated using the standard hydrostatic software [22]. Thus, the virtual roll moment of inertia can be calculated using

$$I_r = (\frac{T_n}{2\pi})^2 \Delta g \overline{GM}$$

where g=9.81 m/s^2.

TABLE I. PARAMETERS OF THE STUDIED ASC

Length $\times$ Width	1.5 m $\times$ 1.0 m
Displacement Δ	163.4 kg
Roll natural period T_n	2.01 s
Roll natural frequency ω_n	3.126 rad/s
Metacentric height $\overline{GM}$	0.2961 m
Virtual roll moment of inertia I_r	48.76 $kg \cdot m^2$

The roll restoring moment (righting moment) parameters i.e. R_i (i=1,3,...) in Eq. 3 can be identified based on the data collected from the vehicle 3D model hydrostatics analysis. Fig. 2 depicts this parameter fitting results where a 3rd order polynomial fitting can provide us with a relatively good fitting results. The identified restoring moment parameter values are R_1=499.13 $N \cdot m$ and R_3=-792.46 $N \cdot m$, respectively.

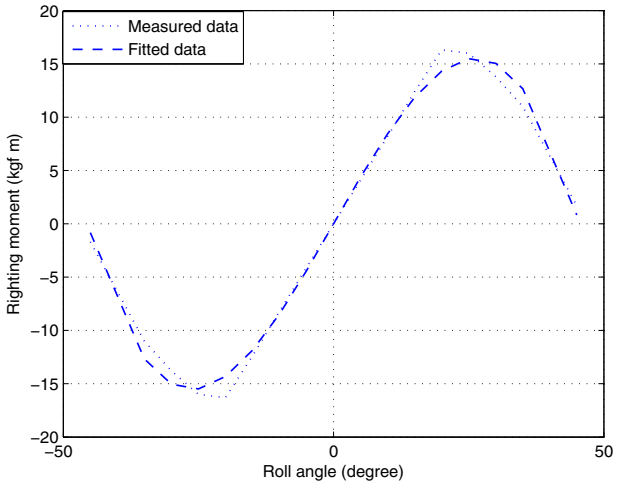

Fig. 2. The 3rd order polynomial fitting of the roll restoring moments compared with the measured data. The data fitting range is in $\phi \in [-45^{\circ}, 45^{\circ}]$.

The energy method [23] has been used for identification of the nonlinear damping terms in Eq. 2. The nonlinear damping effect is evident with large roll motions, thus we choose to use the experimental data set where we have a relatively large ASC roll oscillations for the parameter identification. The decaying curve for vehicle's roll motion can be fitted as an exponentially damped sinusoidal solution [24] with the form

$$\phi = A_m e^{-\sum_{i=1}^{N} \beta_i t^i} cos(\omega_d t + \delta) \tag{9}$$

where A_m and δ depend on the initial condition in the performed experiment and they have been determined as 10.43° and 0, respectively. The damped oscillatory frequency ω_d can be regarded with the same value of the system natural roll frequency assuming the damping effect is small. β_i (i=1,2,...) represent the decay terms. The value of the decay terms can be identified by using the measured maximum positive roll angle in each roll decay cycle. A 3rd order decaying polynomial of β_i has been identified using the least squares method, and the results are given as [β_1,β_2,β_3]=[0.1507,-0.0049,0.0001]. In the roll decay process, the total energy at each time instant t_j can be formulated as

$$\begin{aligned} E(t_j) &= E_{kt_j} + E_{pt_j} \\ &= \frac{1}{2} I_r \dot{\phi}^2 + \int_0^{t_j} (R_1 \phi + R_3 \phi^3) \dot{\phi} dt \end{aligned}$$

where E_{kt_j} represents the kinetic energy and E_{pt_j} stands for the potential energy due to the rolling motion. The total energy will decrease due to the damping forces, and thus the reduction of the total energy in a specific time range will be equal to the negative of the work that is done by the damping forces.

This relationship has been summarized in

$$E(t_{j+1}) - E(t_j) = -\int_{t_j}^{t_{j+1}} (D_1\dot{\phi} + D_2\dot{\phi}|\dot{\phi}|)\dot{\phi}dt$$
$$= -D_1\int_{t_j}^{t_{j+1}} \dot{\phi}^2 dt - D_2\int_{t_j}^{t_{j+1}} \dot{\phi}^2|\dot{\phi}|dt. \quad (10)$$

In Eq. 10, $\dot{\phi}$ can be calculated based on Eq. 9, and the numerical integration is calculated using Euler Method. Therefore, the only unknown terms of D_1 and D_2 can be identified by performing the least squares fitting, and the results are D_1=6.88 $kg \cdot m^2/s$ and D_2=14.63 $kg \cdot m^2$, respectively. We substitute all the identified parameter values into Eq. 1 and perform the simulation in time domain neglecting the wave exciting moments. The comparison depicted in Fig. 3 shows a very good agreement with the experimental data.

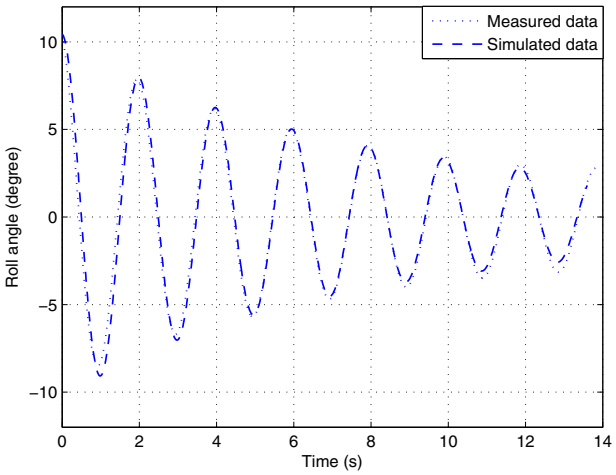

Fig. 3. A comparison between the measured and simulated roll motion. The simulated roll model is without the exciting moments and the unknown parameters have been successfully identified based on the previous analysis.

III. RISK ANALYSIS

The erosion basin or safe basin is a numerical method that has been widely used in analysing marine vessel's roll stability [14], [15]. In this section, we analyse the ASC's nonlinear roll motion based on this technique. For convenience of the following discussion, a non-dimensional form representation of the roll motion model (Eq. 1) has been formulated as

$$\ddot{\phi} + \sigma_1\dot{\phi} + \sigma_2\dot{\phi}|\dot{\phi}| + \phi - \alpha\phi^3 = f(t')$$

where the second and first-order derivative are with respect to the new time scale $t' = \omega_n t$, and the other terms are defined as

$$\omega_n = \sqrt{\frac{R_1}{I_r}},\ \sigma_1 = \frac{D_1\omega_n}{R_1},\ \sigma_2 = \frac{D_2}{I_r},\ \alpha = -\frac{R_3}{R_1}$$

$$f(t') = k_0\cos(\Omega_e t'),\ k_0 = \frac{K_0}{R_1},\ \Omega_e = \frac{\omega_e}{\omega_n}$$

where k_0 is defined as the non-dimensional roll excitation amplitude. It is important to notice that as a lumped parameter k_0 (K_0) already takes into account the wave direction information according to Eq. 8.

While implementing the erosion basin method, the studied phase plane area will be divided into equal sized small grids, and the center of each grid is regarded as a particular initial condition, i.e. initial roll angle and angular rate, for the roll motion simulation. The numerical solution is calculated based on all possible initial conditions. Based on the boundedness of each simulated solution, different zones of safe and unsafe initial conditions in the phase plane can be determined. In this study, the graphs only plot the safe zones. If we vary the wave excitation amplitude, we can investigate the process of the safe basin erosion.

The basin erosion process for a particular example has been depicted in Fig. 4. In this series of simulation, the wave encounter frequency is defined as ω_e=2.6 rad/s and the non-dimensional roll excitation amplitude, k_0, is varied from 0 to 1.8. In each plot, the studied roll motion area is $\phi \in [-80°, 80°]$ and $\dot{\phi} \in [-80°/s, 80°/s]$ and it has been divided into 161×161 equal sized grids. The center of each grid is used as the initial condition for the integration and the simulation time is defined as 100 s. The numerical solution is solved by using the fourth-order Runge-Kutta algorithm. After the integration, if the final roll motion converges to the vicinity of the upright roll position i.e. $(\phi, \dot{\phi}) = (0°, 0°/s)$, this initial condition is safe and will be plotted out in the final phase plane. Otherwise, if the simulation indicates the divergence, that initial condition is unsafe and will be left blank. It shows clearly in Fig. 4 that with the increment of k_0, the boundary becomes fractal and shrinks fast at some point. There are actually two trends in the figure. When $k_0 \in [0, 1)$, the safe basin will reduce from all directions simultaneously. Whereas, if $k_0 \geq 1.0$, the safe basin is eroded irregularly. In other words, even the area that is close to the upright position turns to unsafe region.

To demonstrate this tendency, we generate a plot based on the proportion of the safe initial conditions. When there is no exciting moments, the safe region or the safe initial points reach the maximum number N_m. In the simulation where there is wave excitation, we summarize the number of the safe points N_s and normalize it by N_m, and we call this division the safe region proportion. This result has been depicted in Fig. 5. It can be concluded that the safe region starts to shrink around $k_0 = 0.6$, but it shrinks slowly until $k_0 = 1.0$. When $k_0 > 1.0$, the safe region reduces in a faster rate. This phenomenon is clearly indicated by the last two plots in Fig. 4, and it has been suggested by [25] that the system chaos may have occurred.

The safe region proportion N_s/N_m can be employed for representation of an ASC's rolling motion safety. With the increment of the wave exciting amplitude or the sea states, the safe region will reduce, which indicates a more severe operational environmental condition for an ASC. To examine the relationship between N_s/N_m and the wave encounter frequency, more erosion basin simulations have been performed. A summary of these results have been provided in Table II. We plot the data in Cartesian coordinates as shown in Fig. 6, where the x and y axes are the wave encounter frequency and k_0, respectively and z axis is the safe region proportion. It can be seen that when $k_0 < 0.5$, the safe region will not reduce a lot, but with the increment of k_0 the basin erosion becomes

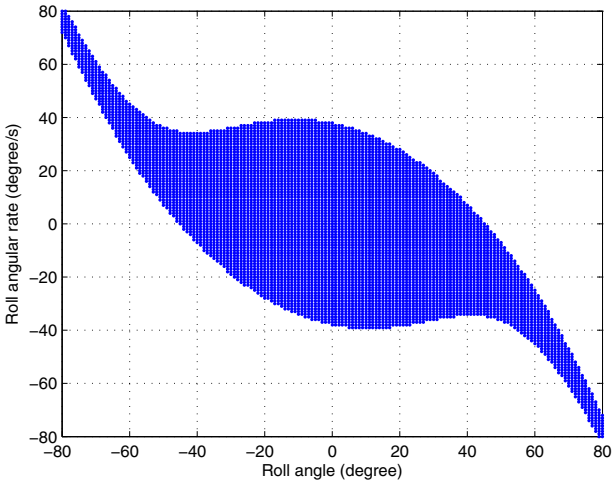

(a) k_0=0

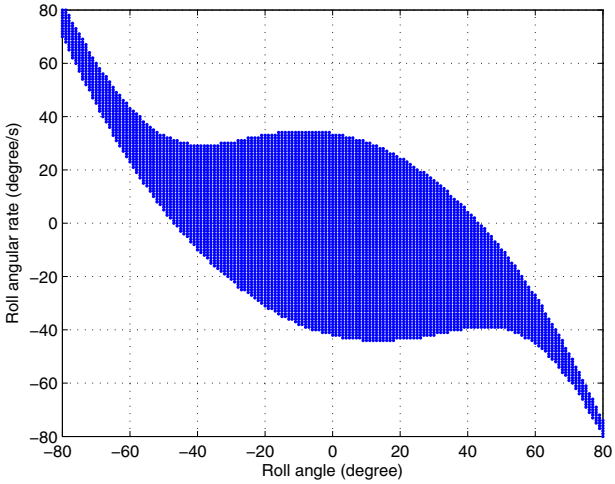

(b) k_0=0.8

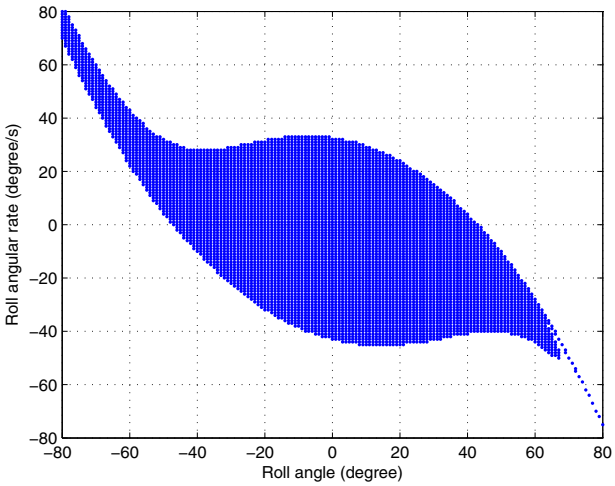

(c) k_0=1.0

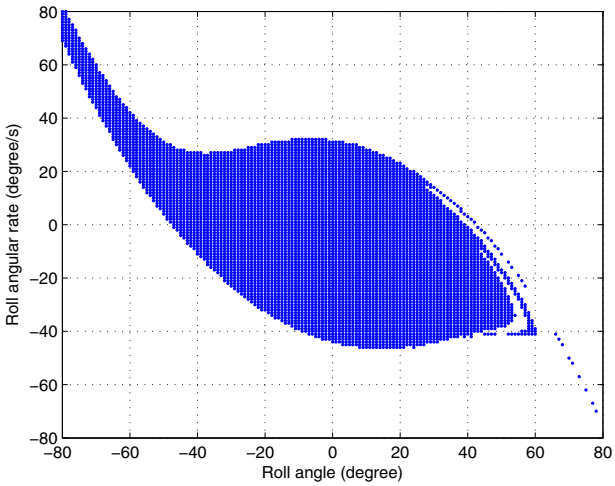

(d) k_0=1.2

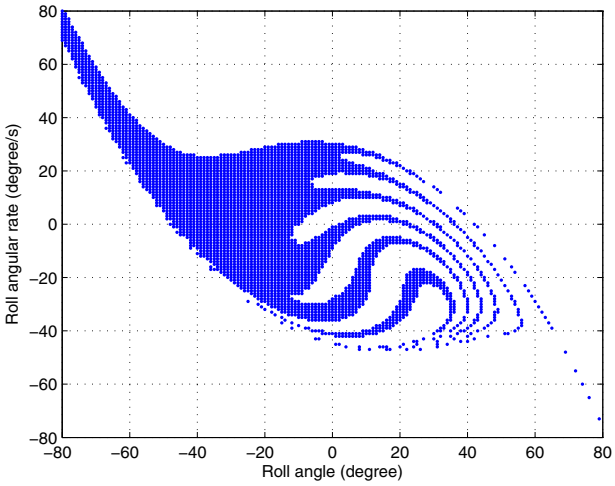

(e) k_0=1.4

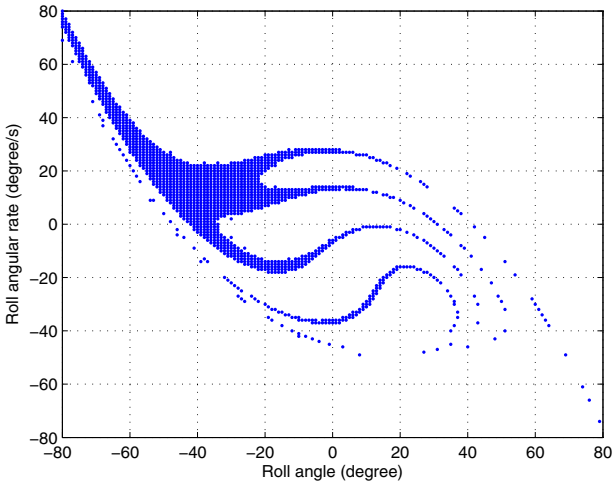

(f) k_0=1.8

Fig. 4. Erosion basin of the dynamic roll motion with the assumed wave encounter frequency of ω_e=2.6 rad/s or $\Omega_e = 0.8334$. k_0 is the non-dimensional roll exciting amplitude.

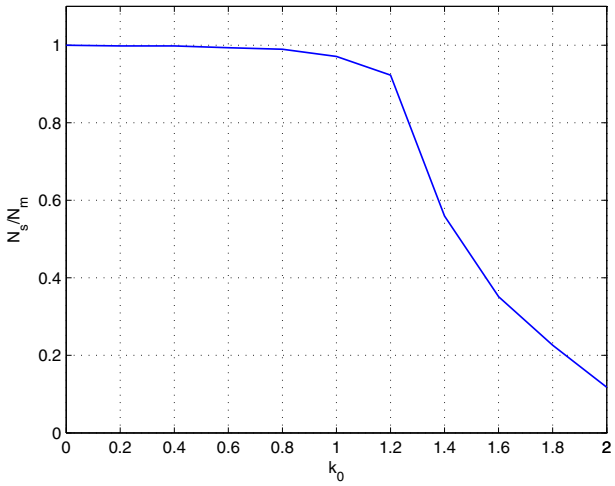

Fig. 5. The proportion of the safe region versus the non-dimensional wave excitation amplitude k_0 when the encounter frequency is 2.6 rad/s.

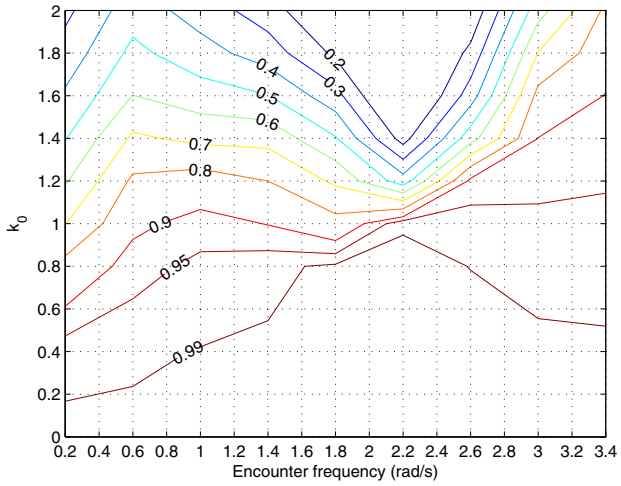

Fig. 7. The contour plot of the safe region proportion with respect to wave encounter frequency ω_e and non-dimensional wave exciting amplitude k_0.

more evident. The worst case is when the wave encounter frequency is around 2.2 rad/s, which features the fastest decrement among all the simulations. Based on Table II, the contour plot has also been generated as shown in Fig. 7. The number on each contour represents the safe region proportion. Again, the wave encounter frequency around 2.2 rad/s marks the quickest reduction of the safe region which is an adverse condition for an ASC to operate.

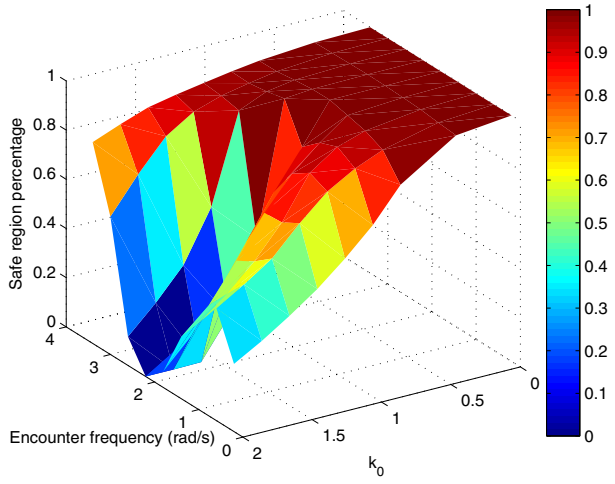

Fig. 6. The safe region proportion versus k_0 and the wave encounter frequency.

The contour plots provide a useful reference for risk analysis of an ASC. For example, assuming an ASC is currently operating in the ocean with a narrow-banded wave spectrum and the peak wave encounter frequency is 0.8 rad/s. Referring to Fig. 7, if the 0.9 contour has been chosen as its roll motion critical boundary, when k_0 >1, the safe region proportion will reduce below 0.9. It also shows that when k_0 >1.4, the safe region shrinks below 0.7 where the fractal boundary may occur (recall the last three plots in Fig. 4), and there is a higher probability that an ASC will capsize through rolling.

It is important to note that the safe region proportion does not explicitly define the probability of capsizing through rolling. However, choosing a specific contour can assist us to evaluate the varying tendency of the ASC safety with respect to different wave encounter frequencies and wave amplitudes (sea states). This is of great importance for risk analysis of an ASC for a specific ocean exploration mission.

The boundary contour can be chosen based on the risk that we want an ASC to take in a specific mission. If we want to be as conservative as possible, it is better to employ the contour of safe region proportion 0.99. However, this choice will make an ASC especially alerted, since the bearable wave amplitude is quite low which might limit the ASC's applicable environments. On the other hand, if the contour of 0.5 has been chosen, although a heavy sea operation is possible, there is a relatively high probability that the ASC will capsize during the mission. Therefore, it is essential for us to choose the boundary contour that can balance the vehicle safety and the possible application scenarios with different sea states.

The contours shown in Fig. 7 have been achieved off-line according to the ASC's roll motion model and extensive simulations. Therefore, it is possible that the tabulated boundary contour data can be integrated into an ASC's onboard guidance and control system to aid an ASC's self safety assessment. For real-time decision making, the ASC has to be able to determine the current ocean environments i.e. wave frequency and wave amplitude, which can either be directly measured by appropriate sensors or be acquired from other sources such as a wave buoy.

IV. CONCLUSION

This paper introduces a risk analysis method for an ASC's oscillatory roll motion in the seaway. The presented method is based on the erosion basin technique, and the roll motion model parameters are identified through using the hydrostatic software and performing the free decay tests in the tank.

TABLE II. SAFE REGION PROPORTION UNDER DIFFERENT WAVE ENCOUNTER FREQUENCIES AND NON-DEIMENSIONAL EXCITING AMPLITUDES

ω_e \ k_0	0	0.4	0.8	1.0	1.2	1.4	1.6	1.8	2.0
0.2	1.0000	0.9761	0.8324	0.6971	0.5897	0.4946	0.4139	0.3405	0.2754
0.6	1.0000	0.9831	0.9296	0.8827	0.8170	0.7168	0.6019	0.5252	0.4572
1	1.0000	0.9916	0.9626	0.9255	0.8482	0.6755	0.5451	0.4413	0.3534
1.4	1.0000	0.9954	0.9805	0.8974	0.8000	0.6695	0.5032	0.3505	0.2495
1.8	1.0000	0.9987	0.9980	0.8354	0.6822	0.5084	0.3365	0.1797	0.0663
2.2	1.0000	0.9997	0.9970	0.9874	0.4467	0.1586	0.0013	0	0
2.6	1.0000	0.9982	0.9896	0.9711	0.9226	0.5592	0.3512	0.2263	0.1176
3	1.0000	0.9966	0.9795	0.9605	0.9378	0.9011	0.8301	0.7036	0.5605
3.4	1.0000	0.9950	0.9782	0.9630	0.9448	0.9253	0.9028	0.8628	0.8185

Extensive simulations indicate the relationship between an ASC's roll motion safety and the wave conditions i.e. wave encounter frequency and wave exciting amplitude. Our future work includes the integration of our analysis results into an ASC's autonomous guidance system to provide an ASC with self safety determination capability. We also plan to extend our analysis to an ASC's pitch and heave motion and combine our results to generate a complete risk analysis strategy.

ACKNOWLEDGMENT

This work is supported by the Natural Sciences and Engineering Research Council (NSERC) through the NSERC Canadian Field Robotics Network (NCFRN). This work is also supported by Memorial University of Newfoundland, by Canada through the Atlantic Canada Opportunities Agency, the Government of Newfoundland and Labrador, the Research and Development Corporation of Newfoundland and Labrador, the Marine Institute and Suncor Energy.

REFERENCES

[1] J. Manley, "Development of the autonomous surface craft ACES," in *OCEANS '97. MTS/IEEE Conference Proceedings*, vol. 2, Oct. 1997, pp. 827–832.

[2] M. Caccia, R. Bono, G. Bruzzone, G. Bruzzone, E. Spirandelli, G. Veruggio, A. Stortini, and G. Capodaglio, "Sampling sea surfaces with SESAMO: an autonomous craft for the study of sea-air interactions," *IEEE Robotics Automation Magazine*, vol. 12, no. 3, pp. 95–105, Sep. 2005.

[3] W. Naeem, T. Xu, R. Sutton, and A. Tiano, "The design of a navigation, guidance, and control system for an unmanned surface vehicle for environmental monitoring," *Proceedings of the Institution of Mechanical Engineers, Part M: Journal of Engineering for the Maritime Environment*, vol. 222, no. 2, pp. 67–79, Jun. 2008.

[4] T. Huntsberger, H. Aghazarian, A. Howard, and D. C. Trotz, "Stereo vision based navigation for autonomous surface vessels," *Journal of Field Robotics*, vol. 28, no. 1, pp. 3–18, Jan. 2011.

[5] A. Pascoal, P. Oliveira, C. Silvestre, L. Sebastiao, M. Rufino, V. Barroso, J. Gomes, G. Ayela, P. Coince, M. Cardew, A. Ryan, H. Braithwaite, N. Cardew, J. Trepte, N. Seube, J. Champeau, P. Dhaussy, V. Sauce, R. Moitie, R. Santos, F. Cardigos, M. Brussieux, and P. Dando, "Robotic ocean vehicles for marine science applications: the European ASIMOV project," in *OCEANS 2000 MTS/IEEE Conference and Exhibition*, vol. 1, 2000, pp. 409–415 vol.1.

[6] M. Caccia, G. Indiveri, and G. Veruggio, "Modeling and identification of open-frame variable configuration unmanned underwater vehicles," *IEEE Journal of Oceanic Engineering*, vol. 25, no. 2, pp. 227–240, Apr. 2000.

[7] C. R. Sonnenburg and C. A. Woolsey, "Modeling, Identification, and Control of an Unmanned Surface Vehicle," *Journal of Field Robotics*, vol. 30, no. 3, pp. 371–398, May 2013.

[8] K. J. Spyrou and J. M. T. Thompson, "The Nonlinear Dynamics of Ship Motions: A Field Overview and Some Recent Developments," *Philosophical Transactions: Mathematical, Physical and Engineering Sciences*, vol. 358, no. 1771, pp. 1735–1760, Jun. 2000.

[9] B. Cotton and K. J. Spyrou, "AN EXPERIMENTAL STUDY OF NONLINEAR BEHAVIOUR IN ROLL AND CAPSIZE," *International Shipbuilding Progress*, vol. 48, no. 1, pp. 5–18, Jan. 2001.

[10] M. N. Hamdan and T. D. Burton, "On the Steady State Response and Stability of Non-Linear Oscillators Using Harmonic Balance," *Journal of Sound and Vibration*, vol. 166, no. 2, pp. 255–266, Sep. 1993.

[11] J. Guckenheimer and P. J. Holmes, *Nonlinear Oscillations, Dynamical Systems, and Bifurcations of Vector Fields*, 1st ed. New York: Springer, Feb. 2002.

[12] J. M. Falzarano, S. W. Shaw, and A. W. Troesch, "Application of global methods for analyzing dynamical systems to ship rolling motion and capsizing," *International Journal of Bifurcation and Chaos*, vol. 02, no. 01, pp. 101–115, Mar. 1992.

[13] W. Wu and L. McCue, "Application of the extended Melnikov's method for single-degree-of-freedom vessel roll motion," *Ocean Engineering*, vol. 35, no. 1718, pp. 1739–1746, Dec. 2008.

[14] I. Senjanovic, G. Cipric, and J. Parunov, "Survival analysis of fishing vessels rolling in rough seas," *Philosophical Transactions of the Royal Society of London A: Mathematical, Physical and Engineering Sciences*, vol. 358, no. 1771, pp. 1943–1965, Jun. 2000.

[15] Z.-J. Long, S.-K. Lee, and J.-Y. Kim, "Estimation of survival probability for a ship in beam seas using the safe basin," *Ocean Engineering*, vol. 37, no. 4, pp. 418–424, Mar. 2010.

[16] J. M. T. Thompson, "Loss of Engineering Integrity due to the Erosion of Absolute and Transient Basin Boundaries," in *Nonlinear Dynamics in Engineering Systems*, ser. International Union of Theoretical and Applied Mechanics. Springer Berlin Heidelberg, 1990, pp. 313–320.

[17] J.-J. Slotine and W. Li, *Applied Nonlinear Control*, 1st ed. Englewood Cliffs, N.J: Prentice Hall, Oct. 1990.

[18] M. Bikdash, B. Balachandran, and A. Navfeh, "Melnikov analysis for a ship with a general roll-damping model," *Nonlinear Dynamics*, vol. 6, no. 1, pp. 101–124, Jul. 1994.

[19] J. N. Newman, *Marine hydrodynamics*. Cambridge, Mass.: MIT Press, 1977.

[20] V. L. Belenky and N. B. Sevastianov, *Stability and Safety of Ships: Risk of Capsizing*, second edition edition ed. Jersey City, NJ: The Society of Naval Architects and Marine Engineers, Jan. 2007.

[21] Z. Li and R. Bachmayer, "The development of a robust Autonomous Surface Craft for deployment in harsh ocean environment," in *Oceans - San Diego, 2013*, Sep. 2013.

[22] "Hydrostatics and Stability Orca3d Naval Architecture Software." [Online]. Available: http://orca3d.com/modules/hydrostatics-and-stability/

[23] J. B. Roberts, "Estimation of nonlinear ship roll damping from free-decay data," Jun. 1983.

[24] R. V. Wilson, P. M. Carrica, and F. Stern, "Unsteady RANS method for ship motions with application to roll for a surface combatant," *Computers & Fluids*, vol. 35, no. 5, pp. 501–524, Jun. 2006.

[25] J. M. T. Thompson, R. C. T. Rainey, and M. S. Soliman, "Ship Stability Criteria Based on Chaotic Transients from Incursive Fractals," *Philosophical Transactions: Physical Sciences and Engineering*, vol. 332, no. 1624, pp. 149–167, Jul. 1990.